Global Advanced Research Journal of Microbiology (ISSN: 2315-5116) Vol. 8(1) pp. 020-034, January, 2019 Issue.
Available online http://garj.org/garjm

Full Length Research Paper

Evaluation of the Withdrawn Water Volume from the Aquifer System of the Spatientrional Sahara

A. Kadria[1*] and Z. Lachiri[2]

[1]Researcher in the Department of Physical Engineering and Instrumentation at the National Institute of Applied Sciences and Technology, the North Urban Area BP 676-1080 Tunis, Personal address: Abu Raihan Bairuni Bukornine Street, 130. Hammam-Lif 2050 Ben Arus Tunisia
[2]Professor of image processing at the National School of Engineering of Tunis, Department of Electrical Engineering, Universal Campus, BP 37 Belvedere, Tunis, Tunisia.

Accepted 15 January, 2019

The present report shows the contribution of remote sensing to estimate the volume of water withdrawn from aquifers, for a semi-arid or arid climate, such as that in our study area: the Aquifer System of Spatientrional Sahara. The vegetation area was firstly estimated from a spatial distribution of vegetation indices from the MOD13Q1 product of the MODIS sensor for a period from 2001 to 2011, by an algorithm highlighting the pixels in the red and the infrared. It's, on average, almost constant at 500 km^2 for all the years. Furthermore, evapotranspiration was defined spatially and statistically by the MOD16A2 product, on the whole basin for 2011. The statistics are derived from an algorithm ensuring the logic based on the Penman-Monteith equation. These statistics regarding the area of vegetation gave the annual total volume of withdrawn water because this volume is evaporated in the absence of rainfall in the water balance and the depth of the basin does not allow it to vary in the ground's level. There was extraction more than 2,5 billion meters-cube. This means that the enormity of the consumption that is, indeed, a few hundred m^3/s. It presents a serious risk of salinity and flow reversal towards the sea. Such a calculation is developed depending on remote sensing elements such as the spatial and temporal resolutions.

Keywords: Aquifer System, arid climate, MODIS, remote sensing.

INTRODUCTION

This report contributes to the presentation of the Aquifer System of Septentrional Sahara (ASSS) as well as an important transboundary basin and is a part of the geological heritage of North Africa. Then, there will be a mention of the methodology used for the estimation of groundwater withdrawals by remote sensing, selected satellite products, the techniques of extraction of the data, ending with interpretation of results.

Until our days, estimates of water volume withdrawals are made by sensors implanted in specific zones but without remote sensing (made with satellites). However, this presents a serious and enormous risk of ignoring many

*Corresponding Author's Email: ahmed.kadria@yahoo.com

unreported figures not monitored by any administration. This is why we have to see the contribution of the remote sensing across the basin for the calculation of the collected total water volume and comparing with the figures mentioned in the database. Such an operation is tricky because the vegetation is very little compared to the total area of the system where we have an arid climate. Thus, we have to see, firstly, the spatial distribution of the vegetation index for governing the evapotranspiration as a capital factor that must be detected and estimated by remote sensing. Indeed, since the water withdrawals from the groundwater are intended, especially for vegetation, the core of the work is focused on:

- The remote sensing of the vegetation zones.
- The calculation of the total evapotranspiration in the entire ASSS basin.

This is due to the neglect of rainfall because it's so little in the semi-aride or even arid climate of our aquifer system. In the other word, evapotranspiration represents the major part of the quantities of water withdrawn for the irrigation.

1. Justification / Significance / Need of the study

The paper shows the contribution of the remote sensing for monitoring the groundwater and water withdrawals in arid climate without need to any implanted sensor in the study area, and this is because the remote sensing uses satellites. It presents an important and great subject since the greenhouse effect and global warming have become more critical and the ozone hole is expanded. Indeed, we fear that this hole makes the global warming more dangerous and the climate more arid. This subject represents a new revolution for some countries since few years. Monitoring the groundwater and water withdrawals by remote sensing touches the totally area of any target study area, especially arid areas. But with implanted small sensors, we cannot touch the totally target zone. Also, it's not easy to install small sensors touching a total desert. So, what to say for a whole continent such as Africa or Australia?! Using satellites is more rapid, too. In addition, the calibration of small sensors short time steps compared to those of the satellite sensors' one. In fact, satellites give results more exact. We'll see that this paper shows the success of monitoring water withdrawals in arid climate by remote sensing, especially in a strategic area shared by three countries: Algeria, Tunisia and Libya, in North Africa. It's a strategic zone because it connects the rest of the continent and it's separated from Europe just by the Mediterranean. The nearer east African zone to Italia is Elhaouria in Tunisia, and the nearer north zone is Bizerte. And any way, by remote sensing we can see corruptions concerning this subject for curing it by new technologies. Indeed, the U.S.A. has a very important machine that gives artificial clouds and moisture, but it requires a compatible initial quantity of water for reactivity with these artificial clouds to result rain. So, the initial quantity depends on zone and climate. We need weather data for this. Also, by remote sensing we can see the critic zones for curing its by pumping great quantities of water to their groundwater from other ones or the sea by desalination. Economically, we can find the cost of the desalination by selling the satellite images.

2. Description of the Northern Sahara's Aquifer System (ASSS)

The ASSS occupies an area of more than one million km^2, of with 700 000 in Algeria, 80 000 in Tunisia and 250 00 in Libya. Its basin (located, of course, at the level of the Earth's crust), has a wide span of 1 800 km E-W and 900 km N-S, with a Tunisian-Libyan coastal plain (The Djeffara) (AYOUB et al., 1981) an important part of the lithosols existing in the world and some form of steppes (especially in the Chotts and in Algeria). This transboundary system is a fossil reservoir (Institut Méditerranéen de l'Eau 2008). It's one of the most exploited basins of the circum-Sahara. It has an outlet (slow because of the braking along the depth of the undergrounds layers) for watersheds existing in the region. The Observatory of the Sahara and the Sahel (Observatoire du Sahara et du Sahel 2003;2003) showed that this transboundary system contains continental deposits in two large groundwater: the "Intercalary Continental" (IC) down in the base (the deepest and most extensive formation, with a temperature exceeding 60°C) and the "Terminal Complex" (TC) at the summit (Figure 1, drawn from the Observatory of the Sahara and the Sahel, 2010).

The IC extends in many hundred meters in depth and its roof is between 50 and 2 300 meters below the surface depending the locations on 600 000 km^2 in sandstones and clays which are 100 to 150 million years old. Fig. 2 (drawn from the Observatory of the Sahara and the Sahel, 2003) shows the geo-location of the ASSS. About 20 000 billion m^3 of water are trapped there. Above, the Sands and Limestone's of the CT formed since 30 to 80 million years ago, contain 11 000 billion more. Their reserves are renewed very little because of the structural configuration and the Saharan climate of the region: These formations are poorly replenished. Indeed, about 1 billion m^3/year in total are infiltrated mainly at the piedmonts of the Saharan Atlas in Algeria, as well as on the Dahar and Djebel Nefussa in Tunisia and Libya. The general structure of the ASSS is presented in three basins:

- The Western Basin, comprising the foggaras sector in the South, the Big Occidental Erg and the Saharan Atlas in the North.
- The Central Basin, the largest in area and depth, with the largest aquifers' thicknesses and the resources are shared by the three countries. Limed to the West by the

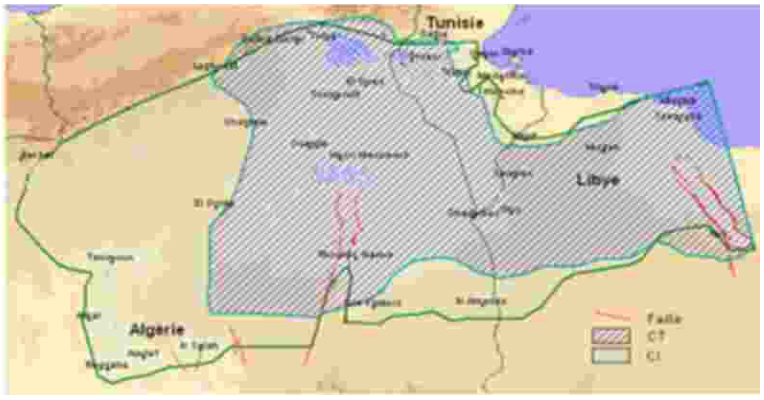

Figure 1: Map, with limitation, of the ASSS basin (Observatory of the Sahara and Sahel, 2010)

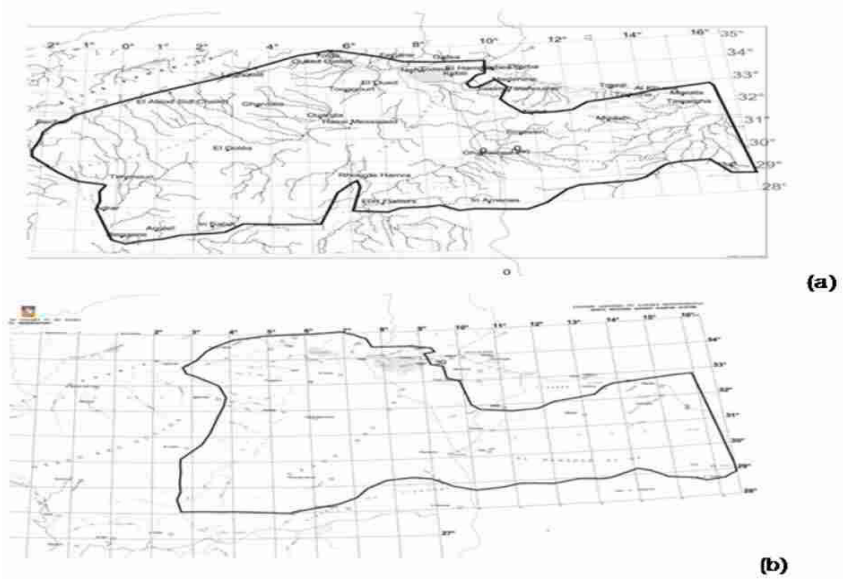

Figure 2: Geo-location of the ASSS for IC (a) and TC (b) respectively (Observatory of the Sahara and Sahel, 2003)

M'zab's Dorsal and to the East by the Highland (Plateau) of **Observatory of the Sahara and Sahel, 2003)**
Hamadah El Hamra, its morphology is dominated by the Big Oriental Erg and the Chotts.

• The Eastern Basin characterized by the collapse of Hun Graben and the accumulation of the tertiary sedimentations.

According to the estimates by the Observatory of the Sahara and the Sahel [3], [4] on the scale of the basin of the ASSS, there would be a total of 30 km^3 of groundwater, of which 10 km^3 would be exploitable with a hydrodynamic balance by continuous drawdown of the water level, for irrigation, drinking water supply and industry (while noting that the exploitable groundwater of the world that have only 1% of the world's freshwater, are 13 million km^3) 80% of these waters are destined for agricultural areas. However, the withdrawals cause a financial problem and a very serious risk of deterioration of the water quality by salinization.

The natural outlets allowed the development of Oasis where the secular lifestyles remained for a long time in perfect symbiosis with the Saharan ecosystem. In 2000, according to the Observatory of the Sahara and the Sahel [3], [4], there were 8 800 water points which are sources and foggaras: 3 500 at the IC and 5 300 at the TC (including 6 500 in Algeria, 1 200 in Tunisia and 1 100 in Libya). In 2008, there were over 18 000 drill holes. Sources are replaced by deeper drilling (some descend more than 1 km). 89 sites (55 at IC) of potential pumping were identified on the entire ASSS (Figure 3).

The lithostratigraphic columns are described in the three countries at different bases:

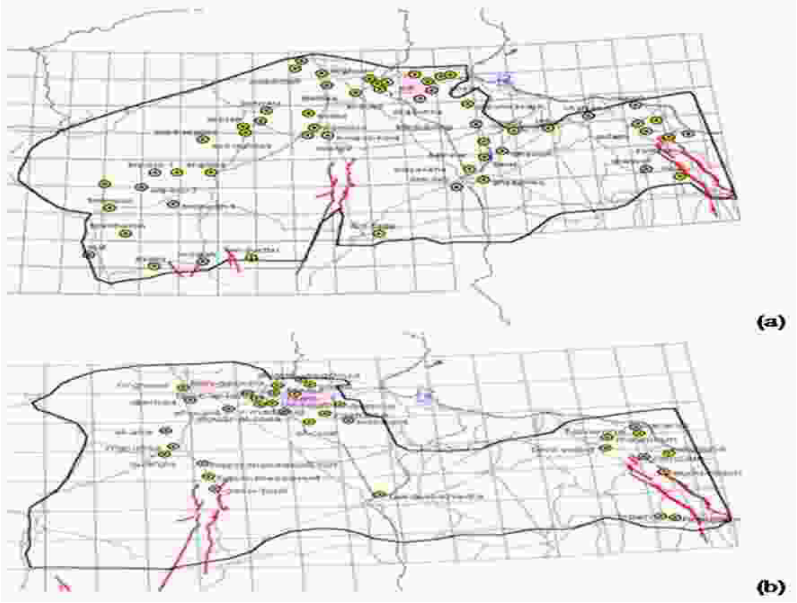

Figure 3: Some potential pumping sites in IC (a) and TC (b) respectively (Observatory of the Sahara and Sahel, 2003)

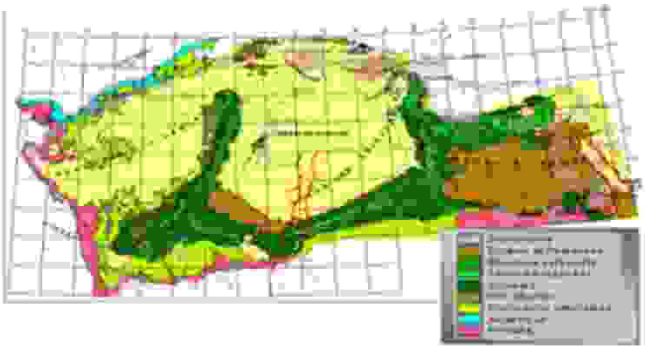

Figure 4: Geological Map of the Northern Sahara (Observatory of the Sahara and Sahel, 2003)

- In Algeria, there are the Triassic, the Lower and Middle Jurassic, the Lower Cretaceous, the Upper Cretaceous and the Continental Tertiary.
- In Tunisia, there are the Upper Jurassic-Lower Cretaceous, the Upper Cretaceous, the Paleocene-Eocene, the Miocene and the Quaternary.
- In Libya, there are the Paleozoic, the Triassic, the Jurassic, the Lower Cretaceous, the Upper Cretaceous, the Paleocene, the Eocene, the Oligocene with Oligo-Miocene and the Mio-Plio-Quaternary (Figure 4, drawn from the Observatory of the Sahara and the Sahel, 2003).

Directly overcome by the Clays of the Cenomanian transgression, the formations of the IC extend to the borders of the northern Saharan platform, in a continuous halo of El Golea to the southern limit of Hamada El Hamra. To the northwest of the basin, the IC is flushed throughout the Saharan Atlas and in N-E on the Dahar and the Jebel Neffusa. Further south, the IC lies directly on the Paleozoic's marine formations, which forms on outcropping a continuous belt from the Moroccan border to the N-W limit of the basin, until the town of Hun in the S-E extreme of the region (Observatoire du Sahara et du Sahel 2003).

Fig. 5 illustrates the west-east section through the ASSS, from the Occidental basin to the Hun Graben (Graben de Hun), and has an exceptional continuity within the sedimentary series of the Saharan platform and indicates the continuity and the homogeneity of the large aquifer formations and of the semi-permeable series. The

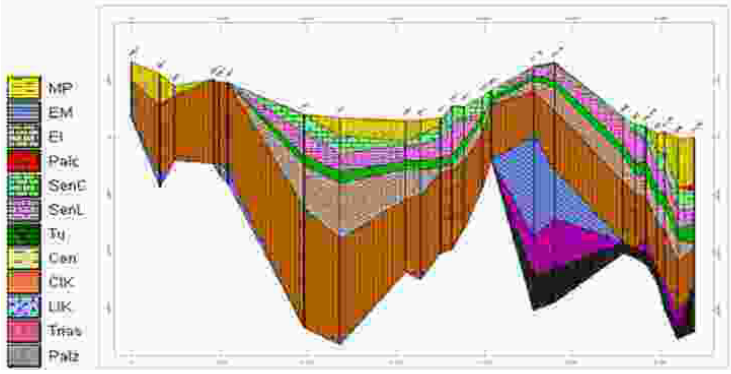

Figure 5: West-East section through the ASSS, from Western basin to Graben Hun (Observatory of the Sahara and Sahel, 2003)

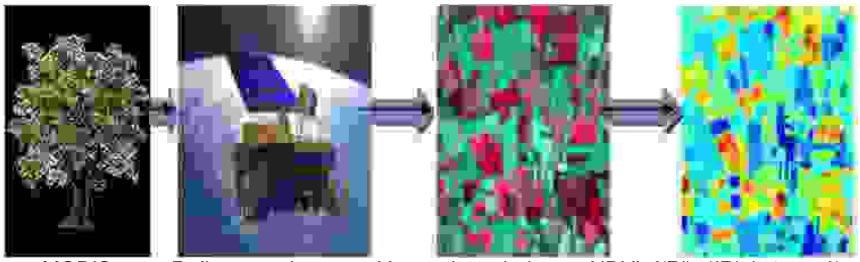

Figure 6: Principle of calculating the vegetation index by MODIS (Bobee and al., 2012)

developed base of geological data allows the automatic drawing of the lithostratigraphic correlations too quickly (because of the high broadband and debit with a very high speed) using the « Rockworks » code.

MATERIAL AND METHODOLOGY

2.1 The MODIS sensor

MODIS (Moderate Resolution Imaging Spectrometer) gives a good estimate of evapotranspiration. This is why we chose to use its data for the case of our study area: ASSS (Huetea et al., 2002; Alfredo et al., 2006).

Among the products that appear to interest in the case of vegetation monitoring at the ASSS:

MOD13Q1: MODIS product dedicated to the NDVI and EVI vegetation indexes, in the form of spectral bands and with a resolution of 250 m, synthesizing the observations of the MODIS/TERRA sensor during a 16 - day revisit period in a heliosynchronous orbit, according to the MODIS algorithm. It also gives the reflectances of the bands 1, 2, 3 and 7. The principle is illustrated as shown in Figure 6 (Cécilia and Milena 2012).

It will be seen that the significant results show that the water flow by the withdrawals from the ASSS is a few hundred m^3/s, which is enormous. These results are obtained from the satellite images of the MOD16 product (belonging to the MODIS sensor) and by deduction of the satellite images of the MOD13Q1 product which give the vegetation area.

2.2 Extraction of vegetation zones

It is important to note that TERRA products use:

2.2.1 Vegetation indexes

The maps show the distribution of vegetation in the ASSS region according to the values of the NDVI vegetation index. Fig. 7 shows the spatialization and the limitation of the ASSS region from the server after accessing http://reverb.echo.nasa.gov/reverb/#utf8=%E2%9C%93&spatial_map=satellite&spatial_type=rectangle.

Figure 7: Spatialization and limitation of the region of ASSS from the server

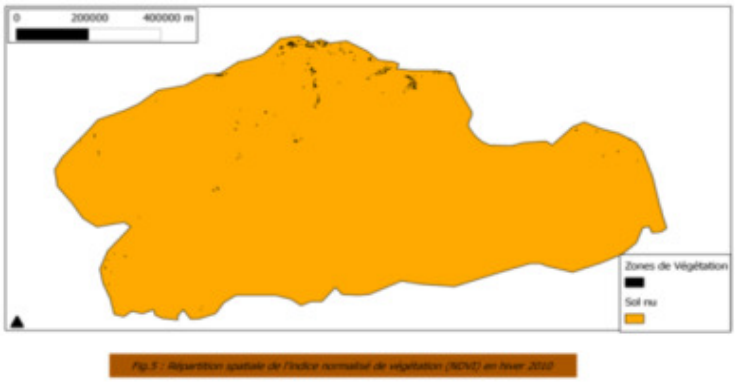

Figure 8: Spatial distribution of the normalized vegetation index (NDVI) in winter 2010 (MOD13Q1 of MODIS)

2.2.2 Data extraction technique

Data processing was done using the two software "ENVI 4.7" (EXELIS Visual Information Solutions EVIS 2012). (Mathieu 2014). and "Quantum GIS (1.8.0)".
Therefore, in order to extract the vegetation zones of the ASSS for different periods, the following steps were carried out:
a / From "ENVI 4.7", the reflectance was drawn from the different tiles in the blue, red, near and mid-infrared bands, and the two vegetation indexes EVI and NDVI.
b / By the same software, the plant areas were segmented, for values of NDVI and EVI between 0,35 and 0,80, because the vegetation, according to Google Earth, appears important only for such thresholding.
c / The plant areas of the region of the ASSS were subsequently polygonized using the "Quantum GIS" software, with the NDVI values (1 revisit/ 16 d). That's in all 253 values. These values show plant distributions better than the values of EVI because NDVI is given directly from the pixels of the matrix image, whereas it is not the case of EVI, which is only given by moving away from the band of the mid-infrared where the MODIS resolution is even lower (500 m instead of 250-300 m). Indeed, it is recalled that:
The normalized difference vegetation index is given by:

$$NDVI = \frac{PIR-R}{PIR+R} \qquad (1)$$

PIR: value of the pixel in the near infrared; *R*: value of the pixel in the red.
The enhanced vegetation index is given by:

$$EVI = G \cdot \frac{\gamma_{\mathrm{NIR}}-\gamma_{\mathrm{red}}}{\gamma_{\mathrm{NIR}}+C_1\gamma_{\mathrm{red}}-C_2\gamma_{\mathrm{blue}}+L} \qquad (2)$$

where γ_{red}, γ_{NIR} and γ_{blue} are the reflectances in the red (645 nm), near infrared (860 nm) and blue (469 nm), respectively, and correspond to the bands 1, 2, and 3 of MODIS. G, C_1, C_2 and L are useful parameters to represent the diffusion of aerosol and the absorption, and their values are 2,5, 6, 7,5 and 1 respectively (Adrian et al., 2009; (NASA LP DAAC, USGS EROS Center and Sioux Falls 2013).
Fig. 8 (MOD13Q1 of MODIS) shows an example illustrating the plant distribution in winter of the year 2010 according to the NDVI values. The image of the spatial distribution of

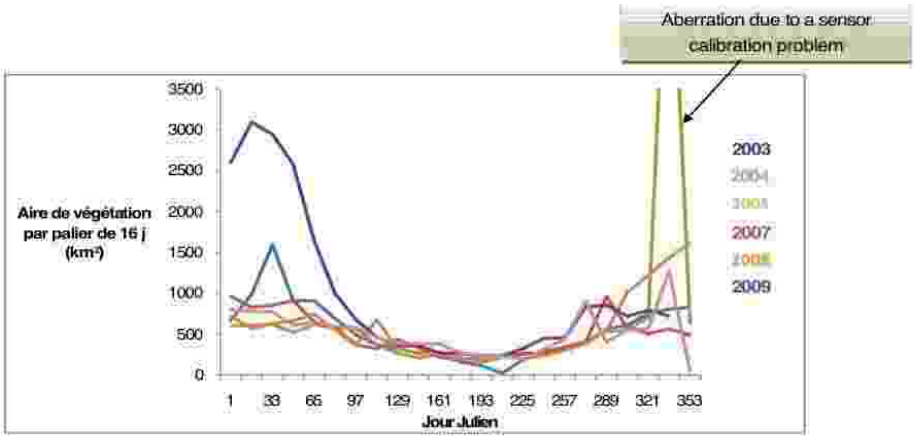

Figure 9: Vegetated areas in the ASSS during the last decade

Figure 10: A potato crop (Observatory of the Sahara and Sahel, 2013)

the normalized difference vegetation index (NDVI) is panchromatic because our goal is not the change in NDVI, but the calculation of the vegetated area that would allow us to show the contribution of the remote sensing for the estimation of the water volume withdrawn from the aquifers of a basin having an arid area. We have a low spatial distribution of NDVI because the climate is arid, and therefore, low vegetation.

Fig. 9 shows the variability of the vegetation area in the ASSS during the last decade.

4.2.3 Spatio-interpretation according to the data

Parallel to the data extraction steps, a comparison interpretation from the vegetation indexes was proceeded to recent data whose resolution is lower than 1 m.

There are green canals in the desert, monocultures in farms, oases, olive groves (which are generally planted, for example in southern Tunisia, with a space of about 30 m between the feet), market gardening and some shrubs. Fig. 10 (Observatory of the Sahara and the Sahel, 2013) and Fig. 11 (Project of Sustainable Management of Oasis's Ecosystems, 2014) show, respectively, a potato crop and a general view of the Chebika oasis and its environment.

The pre-processed and interpreted data made it possible to have an information set covering the period 2001-2011, which is important to analyze spatially and temporally. We have to connect them to a type of land use in order to establish methods of estimating consumed water (sampled from the ASSS).

The intra-annual and interannual variations of vegetation area (Figure 9) are explained, further that the rains are irregular and differently distributed in space, by the presence of natural plants such as herbaceous. These variations are remarkable in winter. In the summer, this is not the case, but there is a vegetable resistance that is probably due to a human activity of irrigation or to exceptional runoff.

Figure 11: General view of the oasis of Chebika and its environment (Project of Sustainable Management of Oasis's Ecosystems, 2014)

Sometimes, we find out the outliers (aberrant values) generated, certainly, by a problem of calibration of the data of MODIS: It is the case of the year 2005.

2.3 Satellite data of evapotranspiration for estimating the volume of withdrawn water

This sub-paragraph is the fundamental challenge to show the contribution of remote sensing and image processing to estimate the quantities of water withdrawn from the aquifer.

The evapotranspiration means the transpiration of water vapor stored in the leaves. It occurs by the stomata's opening. Such a phenomenon is not only biological, but biophysical because the opening of the stomata is a mechanism not occurring randomly. Indeed, for an arid climate, the opening of the stomata is more present because of the need for water that the plants require. The good presence of the plants gives an important evapotranspiration governed by the opening of the stomata. More the stomata are opened, more we have vegetable transpiration. Under good water conditions, the two stomatal cells absorb a significant amount of water, causing their curvature and swelling to result the opening of the ostiole (stomatal orifice). If the air is hot, the ostiole is raised up because of its low mass. This leads the concentration of cold air at lower altitudes (in addition, physically, cold air is lower than warm air because the first one is heavier and therefore more attracted by Earth's gravity). However, the cold air is often accompanied by moisture, and therefore, there is the presence of water's droplets. This causes their absorption by the stomata, and consequently, evapotranspiration. It is recalled that about 10% of the moisture in the atmosphere is released by plant transpiration. During a period of growth, a leaf will transpire much more water than its own weight. The amount of water that plants release varies greatly according to the geography and over time. There is a number of factors that determine transpiration rates:

- Temperature: the rate of transpiration increases with temperature, especially during the period of growth, when the air is warmer.
- Hygrometric degree: If the humidity level of the air that surrounds the plant increases, the rate of transpiration decreases. It is easier for water to evaporate in dry air than in saturated air.
- The movement of the wind and the air: the increase of the movements of the air around the plant will result in a greater transpiration.
- The type of plant: the rates of transpiration depend on the type of plants. Some plants that grow in arid regions, such as the cactus, retain valuable water by transpiring less than other plants.

MODIS data are commonly admitted with the ET (terrestrial evapotranspiration) model to estimate ET_{rs} (rs to say: remote sensed) due to its high radiometric sensitivity, high temporal resolution, high moderate spatial resolution and it is uncharged.

The Penman-Monteith equation is written:

$$ET_{\mathrm{rs}} = \frac{1}{\lambda}\frac{\Delta(R_{\mathrm{n}}-G)+\rho_{\mathrm{a}}C_{\mathrm{p}}DG_{\mathrm{a}}}{\Delta+\gamma\left(1+{}^{G_{\mathrm{a}}}/_{G_{\mathrm{s}}}\right)} \qquad (3)$$

where: λ is the latent heat of vaporization;

$\Delta = (de)^{*}/(dT)_a$: the slope of the relationship between the temperature and the pressure of the saturated water vapor (kPa /°C);

$D = e^{*}(T_a) - e_a$: the vapor pressure released from the air (kPa);

$e^{*}(T_a)$: the saturation vapor pressure at the given temperature of the air;

e_a: the pressure of the current vapor;

γ: the psychrometric constant (kPa/°C);

ρ_a : density of the air (kg/m^3) ;

C_p: Specific calorific capacity of the air;

G: the heat flux of the sun (kJ/m^{2}s);

R_n : radiation nette (MJ/m^{2}j) ; $R_n = R_{ns} - R_{nl}$: difference between the incoming radiation short-wave and the outgoing radiation long wave;
$R_{ns} = (1 - \alpha_c)R_s$ where : α_c is the surface albedo (bleaching) et R_s the solar radiation.
R_{nl} is calculated using the Allen et al method. (1998):

$$R_{nl} = \sigma\left(\frac{T_{max}^4+T_{min}^4}{2}\right)\left(0{,}34 - 0{,}14\sqrt{e_a}\right)\left(1{,}35\frac{R_s}{R_{so}} - 0{,}35\right) \quad (4)$$

where: σ is the Boltzmann constant (4.903.10^{-9} MJ.K^{-4}m^{-2}.d^{-1});
T_{max} and T_{min} are the extrema of the temperatures of the air (K);
R_{so} is the solar radiation through a clear sky;
R_s / R_{so} is the short-wave relative radiation (limited to ≤ 1,0).

k_Q: extinction's coefficient for photo-synthetically active radiation;
k_A: attenuation of all irradiated net waves;
Q_h: the photo-synthetically radiative activity at the top of the canopy;
Q_{so}: value of the absorbed photosynthetic active radiation when $g_s = g_{sx}/2$;
D_o: value of D when g_s is reduced to $g_{sx}/2$;
g_{sx} is the maximum value of g_s.
f: fraction of equilibrium evaporation at the soil surface (from 0 to 1).
We note, therefore, that the satellite estimation of evapotranspiration requires an algorithm which takes into account all the parameters mentioned above, and that the equation of Penman-Monteith includes an energy term and an aerodynamic term. Estimation of evapotranspiration requires good equipment governed by well-calibrated sensors, in order to make good settings and detections with as little loss of information as possible. Such an operation becomes more delicate and complex when the environment knows an accentuated aridity, and this is the case for the ASSS region. Always with the MODIS sensor, this estimation was made from the satellite images of the MOD16 product.

Technique and data processing:

The work began with the download of the MOD16 data on 5 bands:
- ET (evapotranspiration) for 8-day, monthly and annual increments
- LE (latent heat) flux for 8-day, monthly and annual increments

$G = a_1.R_n$ where a_1 is the ratio of the net radiation. a_1 is set at 0,1 according to the measurements of the savannah sites (Cleugh et al.2001).
G_a : aerodynamic conductance that is 1/30 in forests, 1/80 for shrubs (small trees) and 1/100 in the Prairies and cropland.
Lenning et al. (2007) showed that the surface conductance is:

$$G_s = G_c\left\{\frac{1+\frac{\tau G_c}{(1+\varepsilon)G_c}\left[f-\frac{(\varepsilon+1)(1-f)G_c}{G_a}\right]+\frac{G_a}{\varepsilon G_i}}{1-\tau\left[f-\frac{(\varepsilon+1)(1-f)G_c}{G_a}\right]+\frac{G_a}{\varepsilon G_i}}\right\} \quad (5)$$

with: $G_c = \frac{g_{sx}}{k_Q} Ln\left[\frac{Q_h+Q_{so}}{Q_h exp(-k_Q LAI)+Q_{so}}\right]\left(\frac{1}{1+\frac{D}{D_o}}\right)$ (6)

where : $\varepsilon = \Delta/\gamma$;
$G_i = \gamma\ (R_n - G)/\ (\rho_a C_p D)$: isothermal conductance (Monteith and Unsworth 1990);
G_c: cover conductance;
τ = exp(-k_λLAI) : the fraction of the **available transmitted energy** to the bottom of LAI (leaf area index) ;
g_{sx}: maximum stomatal conductance;

- Potential evapotranspiration ETP for 8-day, monthly and annual increments
- the potential flow of latent heat LEP for 8-day, monthly and annual increments
- annuel QC control quality (ET) and for 8-day increments.

For this reason, it is sufficient to select, only, the first band that is extracted from the MOD16A2 products to estimate ET. The data are acquired by an algorithm based on the Penman-Monteith equation which calculates ET [12] and whose schema is as shown in Figure 12 (Qiaozhen et al., 2011).
The program shows that the spatial resolution is 1 km (grid 1 km * 1 km) and that the values of the evapotranspiration are given in mm. This spatial resolution corresponds to the bands 8-36 of the MODIS sensor, that is to say the visible (405 nm corresponding to the violet) to the short waves of the infrared medium, or even the thermal infrared (14,4 µm).

RESULTS AND DISCUSSIONS

Fig. 13 (MOD16A2 of MODIS) shows the northern vegetation, particularly at Djebel Lakhdhar (not far from The Djeffara), and the presence of moisture in the western basin in the southwest of the ASSS in Algeria. In the southeast of the ASSS, the vegetation takes place following the project of water stock and water jet made by the Libyan government. This is shown by the treatment of land-use maps carried out by the Observatory of the Sahara and the Sahel for 11 pilot zones, including that of Jufrah, showing the located vegetation at the level of the Libyan project.

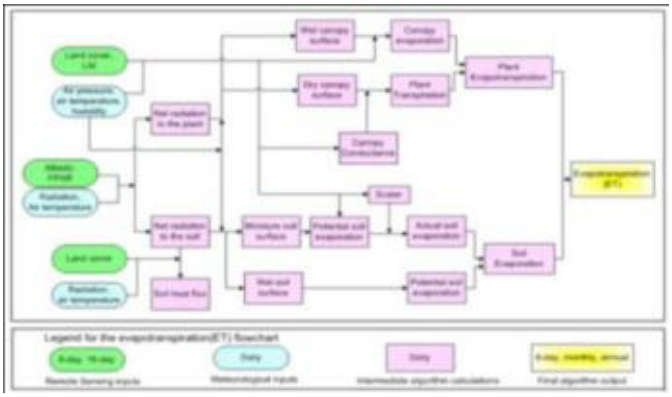

Figure. 12: MOD16 algorithm providing the logic for calculating evapotranspiration ET (Qiaozhen et al., 2011)

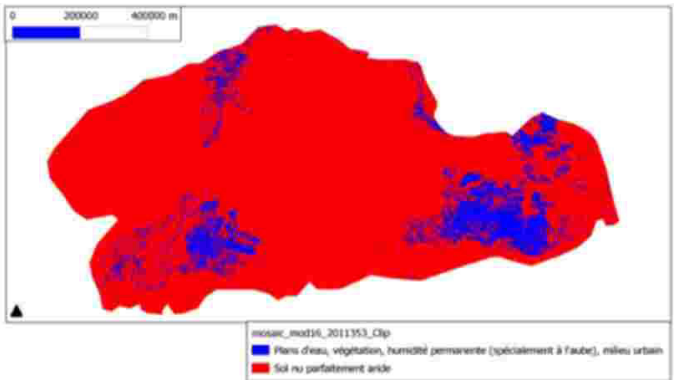

Figure 13: Distribution of evapotranspiration for a bearing of 8 d given in mm for 2011 (Julian day: 353) (MOD16A2 of MODIS)

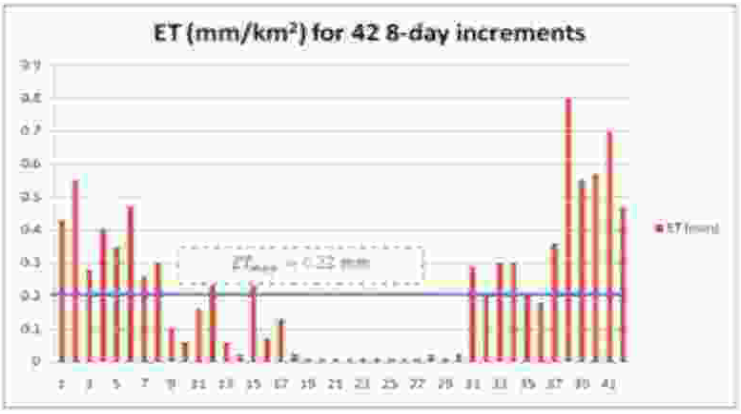

Figure 14 : Change in evapotranspiration for a bearing of 8 d given in mm for 2011

Fig. 14 is obtained from values deduced following a very large zoom-in succession of a sweep affecting the entire vegetation of the area of the ASSS. It shows the change in evapotranspiration for a bearing of 8 days given in mm for the year 2011.

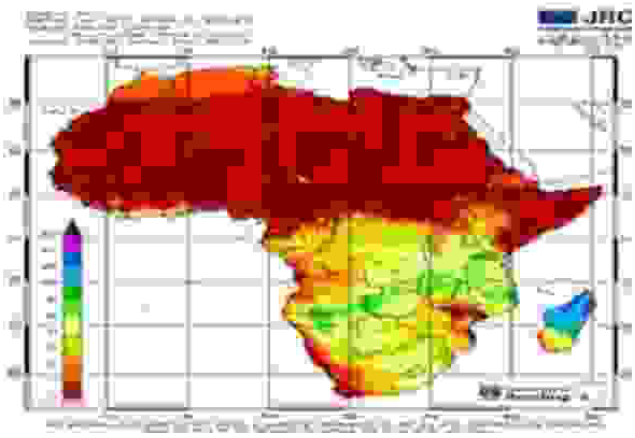

Figure 15: Changes in rainfall given in mm for the first decade in the winter of 2010 in Africa (University of Reading, 2010) (MSG TIR of TAMSAT)

Calculation of the withdrawn water volume:

We put into consideration, for the calculations, for each year, the raster layers of ET that the first knew a fairly high increasing variation (neglecting rainfall and therefore, infiltration due to the verified aridity of the climate). This fairly high variation is estimated as being the result of irrigation, and not of a rain, because during the precipitation, the humid climate prevents the palms transpiring.

Given that the climate is semi-arid and even arid in the entire area of the ASSS, the notorious inadequacy of rainfall, and consequently the infiltration, and the water's variation at the ground level (especially that the basin is deep) are negligible in the total water balance. Fig. 15 (from University of Reading, 2010) (MSG TIR of TAMSAT) shows an example of low quantity of rainfall in North Africa, where the ASSS is located, in winter 2010, and that it is between 0 and 1 mm in the major part of our basin. Then, the samples are almost entirely evaporated by the vegetation, and especially by the palms. Therefore, evapotranspiration is almost the totality of the water balance. Urbanization points, water plans (water bodies) and humidity are excluded from the calculation of the water balance. The spatial resolution of the raster layers gives ET per km^2 (because the resolution is 1 km * 1 km). So, for each km^2, we have one value (one pixel). This allows us to determine the metric amount (in m) of withdrawn water for an 8- day increment by multiplying ET by the number of km^2 affected by the transpiring vegetation. For one year, the metric quantity of withdrawn water (for irrigation) is the sum of the withdrawn quantities of water during N 8-day increments. ET is almost constant in summer (about 0,01 mm for the year 2011). To find the volume V of withdrawn water, it's sufficient to multiply the metric quantity of withdrawn water by the area of transpiring vegetation.

In conclusion, the volume of withdrawn water along a year is given, in m^3, by the equation:

$$V(\mathrm{m^3}) = [\sum_{i=1}^{N} ET_i \left(\mathrm{mm}/\mathrm{km^2}\right) \times 10^{-3} \times \mathrm{area}(\mathrm{km^2})] \times A(\mathrm{m^2})$$

Metric quantity (7)

With,

V: volume of withdrawn water along one year (m^3);

ET: mean evapotranspiration (mm/km^2);

N: number of 8-day increments of evapotranspiration during one year;

A: area of irrigated vegetation (m^2).

It is an equation which represents the contribution of the remote sensing to the estimation of water withdrawals. It shows the effect of the spatial (1 km * 1 km) and the temporal resolutions (8 d), as well as the statistics derived from the satellite images (the values of the evapotranspiration for one year and the vegetation area which's about 500 km^2).

If we choose to calculate the volume from the mean evapotranspiration, it is necessary to multiply this factor (the mean evapotranspiration) by the number of N

increments. In this case, the withdrawn water volume is written:

$$\boldsymbol{V(\mathrm{m^3}) = [ET_{mean}(mm/km^2) \times 10^{-3} \times \text{area}(km^2) \times N] \times A(m^2)}$$

(8) Metric quantity

For the year 2011, as shown in Figure 14, we consider the number N equal to 42 8-day increments giving the raster layers of ET because the previous values of ET are the progression of the conditions of the last days of the last year before and that the rains' quantities are low on day 33, yet there is an evapotranspiration not to be neglected. In other words, the first 3 levels are subtracted because this is the progression in the last levels of the year 2010 (because the first guaranteed variation during the year 2011 was at the fourth level).

By subtracting the effect of moisture at dawn (which gives raindrops to vegetables) and neglecting the effect of precipitation towards the end of the year, the irrigation's estimation is spotted by a rate of an average evapotranspiration of 0,22 mm for the 42 Julian days of the year 2011. Figures 8 and 9 show that the estimation of the vegetation area in the ASSS is about 500 km^2.

As a result, for 2011 and an area of 500 km^2, according to Figure 14 and referring to (7), we can estimate the withdrawn water volume (for irrigation) from the groundwater of the ASSS approximately as:

$$\boldsymbol{V = 9.190 \times 10^{-3} \times 500 \times 500 \times 10^6 = 2.2975\ billion\ \mathrm{m^3}}$$

But since the resolution is low (1 km), it is easy to verify that 2 mm/km^2 can be added and even much more for the total evapotranspiration for all of the year 2011 (and every year of the decade because of the drought and low spatial resolution of the satellite). For a value 11 mm/km^2, the withdrawn volume is 2,750 billion m^3. An enormous result corresponding to the totality of the basin, given that the mathematical model of the database of the Observatory of the Sahara and the Sahel provided, after verification by certain field missions of tens of plots of land and more, a withdrawn volume of 2,736 billion m^3.

For the average evapotranspiration which is 0,220 mm/km^2, we have according to (8): $\boldsymbol{V = 0.220 \times 10^{-3} \times 500 \times 42 \times 500 \times 10^6 = 2.310\ billion\ \mathrm{m^3}}$

Similarly, for an evapotranspiration of 0,250 mm/km^2, we have:

$\boldsymbol{V = 2.625\ billion\ \mathrm{m^3}}$,

And for an evapotranspiration of 0.300 mm/km^2, we have:

$$\boldsymbol{V = 3.150\ billion\ \mathrm{m^3}}$$

These results show the validity of our hypothesis to suppose the negligence of the quantities of rain in the water balance because each year there is generally a hundred mm of precipitation, which presents nothing to the neighborhood of 4,6 m of withdrawn water from the groundwater of the ASSS's basin, We recall that this neighborhood (4,6 m) is given by the metric factor ($9.190 \times 10^{-3} \times 500$), according to (7). Even for the mean evapotranspiration (0,22 mm), there is a withdrawn quantity of water such that, according to (8):

$0.220 \times 10^{-3} \times 500 \times 42 = 4.62\ \mathrm{m}$.

These results also show a danger (hundreds of m^3/s) and a more serious risk compared to estimates made by the OSS (tens of m^3/s). This may reflect the increase in the salinity of the water and the reversal (inversion) of the flow towards the sea (mainly towards The Djeffara) (Adel Kharroubiet al. 2014).

The mathematical estimative model of the database of the Observatory of the Sahara and the Sahel showed that it is 2,300 billion m^3 for the year 2008 and 2,736 billion m^3 as indicated above. This is comparable with the remote sensing model explained above. The data's quality remains to be improved. In addition, we expect that results will be obtained for plots (parts of the ASSS) from very high resolution images, including 11 obtained by SPOT and Quick Bird.

In plots, for example in Kebili, the mean area of vegetation in 2011 is 100,835 km^2 with an average evapotranspiration of 0,300 mm/km^2 obtained by sweeping its area extracted from the evapotranspiration's map on the entire ASSS. This gives us a withdrawn volume of 128112985,035 m^3 (computed by the formula established above ((8)) and whose numerical application is:

$0.3 \times 10^{-3} \times 100.835 \times 42 \times 100.835 \times 10^6 = 128112985.035\ \mathrm{m^3}$).

But this is deduced from the vegetation maps. However, since the satellite is having a medium resolution, and according to the maps of the ET, there are the vegetables that have not been detected. In all, according to what is reported, we have about 152 km^2 of irrigated zones (http://www.tunisieindustrie.nat.tn/en/doc.asp?docid=595&mcat=13&mrub=105). It is a quasi-fixed figure even on 10/02/2017 because the climate and the agriculture correspond to this surrounding. It can be checked by e-mail at dr.kebili@api.com.tn, and it is noted by "Copyright © API Tunisia 2016 - All rights reserved".

But drawing from the vegetation map in union with the map of evapotranspiration as shown in Figure 13, this evapotranspiration's map shows that the forest area of 23 km^2 in Kebili is also irrigated because the rain is too rare and too little, and yet there's evapotranspiration in these forests. As a result, there are 175 km^2 of irrigated zones. From these maps, we deduce, by zooms-forward too advanced on the summation raster layer, that $ET_{average}$ is 0,300 mm/km^2 in 2011 for the Kebili area.

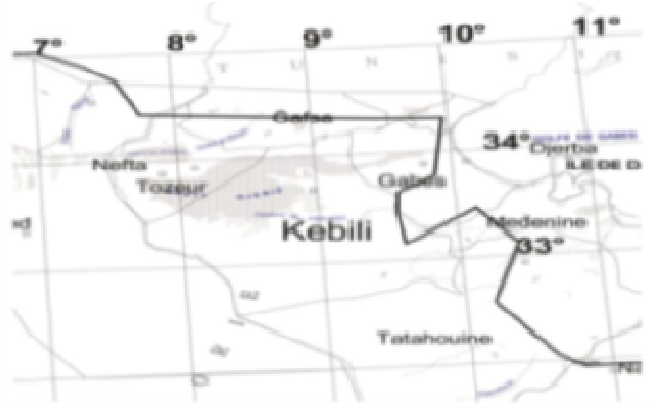

Figure 16: Georeferencing areas of Tozeur and Kebili

Either, a volume of withdrawn water is:
$0.3 \times 10^{-3} \times 175 \times 42 \times 175 \times 10^{6} = \mathbf{385875000\ m^3}$.

However, applying the BD model [3], [4] (see DATABASE AND SIG – Observatory of the Sahara and the Sahel, June 2003), we have in 2011:
Operation CT Kebili: 318387129 m^3
Operation CI Kebili: 42171941 m^3
That is a total of 360559070 m^3.
This remarkable difference on the Kebili plot is probably due to the fact that the database's model of the Observatory of the Sahara and the Sahel did not take into account the evapotranspiration's factor detected by the MOD16A2 sensor.
By the same process, we find that in Tozeur that we have an average evapotranspiration of 14 mm/km^2 in the entire 2011 year. As a result, the withdrawn water volume in Tozeur, according to (7), is:
(14 * 0.001 * 83.465) * 83.465 * 10^6 = **97.53 millions m^3**.
Here are the figures reported by the OSS database for Tozeur for the year 2011:
CI : 3256423
CT : 94859979
CI+CT = 3256423 + 94859979 = **98.116402 millions m^3**
The difference between this value and that provided by the database is probably due to uncertainties and some small defects of calibration, and that the extreme northern part of the governorate of Tozeur does not belong to the ASSS. So, there are points which were excluded during the calculations.
But also, according to field missions, and by confirmation of Wikipedia and some photos of Google Earth, the palm grove is cut into several small grassy gardens.
The cutting of the plots of Tozeur and Kebili is illustrated in georeferencing in Figure 16. The delimitation of the Tozeur zone is made by the Shapefile tozeur_geo.shp . Similarly for Kebili (replacing Tozeur by Kebili).

CONCLUSIONS AND PERSPECTIVES

Among the remarkable types of vegetation, we saw dry agriculture, intensive irrigated agriculture in palms (traditional and modern in stages (structure made by the French)), olive groves, herbaceous lands, wild plants at the level of the Chotts. It is necessary to take into account the heterogeneity of a same type of plant, governed by the dimensions of the feet, the trunks, the leaves and the stomata. However, irrigation waste should also be considered. Generally, wasted irrigation water is stored in drains through which the water passes through the pipeline to get into the undergrounds. The remote sensing, which allows us to know the land use, gives us, among others, water plans. From these plans of water, we can ensure other truth missions in order to follow the tracks and go to the drains to measure the amount of water stored in each one.

By comparing the results with those reported before, we can explain the causes of the evolution of the ASSS's ecosystem. The destruction of important green areas is explained, mainly, by the fortification of housing, the accentuated climate change by drought, and the increase in the water's salinity. The drought and the increase in the water's salinity, in addition to the inversion of the water flow, especially at the level of The Djeffara, were also explained by the obtained results in this article, and which concern the withdrawn volume of water.

The use of very high resolution imagery available on-line through Google Earth appears promising in order to better map land use at the scale of pilot zones or even Oasis. This type of imagery, thus, has a high added value compared to the high resolution data of the SPOT satellites (1st generation SPOT 1-4, 20 m as spatial resolution in multispectral mode). However, an additional methodological work remains to be done in order to estimate water withdrawals by associating to each LU (land use) class theoretical crop coefficients and water volumes for irrigation with, following a Cropwat methodology (FAO Water Development and Management Unit 2013). This methodology does not take into account the losses in the network and the wastage during irrigation.

Nevertheless, the use of the very high spatial resolution meets some limitations:

-1- Coverage: For Quick Bird, for example, the swath is 16,5 km. Also for Ikonos, the swaths are 11-14 km * 11-14 km (range dimensions per picture). It's true that it gives a good view of land use and data in general, but it only affect well-defined plots having the dimensions mentioned above. The coverage does not touch all land.

-2- Frequency of revisiting the same site: The repeatability is generally greater than 2 days. For IKONOS, the temporal resolution is 3-5 d with change of the pointing of its instruments, and every 144 d in nadir (Digital Globe, 2013). For Quick Bird, the revisit frequency is 3-7 days. Additionally, Quick Bird images are provided by Google Earth, and it shows that the data are neither recent nor of the same date. We need a budget of several billion to have a good deal on it, and then improve the quality of the results (images and their comparisons).

-3- Processing time: The very high spatial resolution involves a large volume of data for each image (2 GB/image). Therefore, their processing by photo-interpretation requires a much longer time than that of the automatic or semi-automatic image processing with low and medium spatial resolution.

Moreover, for the sensors of medium spatial resolution, such as those of the sentinel-2 and sentinel-3 of the ESA (European Spatial Agency), which ensured the images following the scanning of the entire planet, are getting to know an evolution of the spatial, temporal and spectral resolutions, before launching them towards the space during the years 2013-2016. There is an improvement in the spatial resolution compared to that of MODIS, but a small weakness in the frequency of revisit and the colors. Indeed, each of the two Sentinel-2 satellites will observe all the emerged lands every 10 days, with a spatial resolution of 10-60 m, in 13 spectral bands (which is not low, even if it is a slightly less than for MODIS) from the visible to the medium infrared. Sentinel-2A should be launched before the end of 2014, and Sentinel-2B 18 months later. With both, they will allow observations of all the emerged lands every 5 days. The data will mainly be used in the areas of land use and others. As for Sentinel-3, this mass satellite of about 1,2 t, based on a new platform derived from PRIMA and PROTEUS, will be equipped with 4 main instruments: OLCI (Ocean and Land Color Instrument), SLSTR (Sea and Land Surface Temprature Radiometer), SRAL (Sar Radar ALtimeter) and MWR (MicroWave Radiometer). OLCI will have a resolution of 300 m, but a wider swath of 1,250 km and a capacity to distinguish 21 colors (whereas MERIS has a capacity to distinguish 15 colors). It is an optical instrument dedicated to the color of the emerged land to ensure, in particular, a monitoring of the state of the coastal zones (pollution, current, ..). This instrument will allow better prediction of changes and better management of its resources. It is an advanced version of the MERIS imaging spectrometer which flies on Envisat (FLASHESPACE, 2010).

Conversely, the hyper-spectral data of the MODIS, SPOT-VEGETATION or SEVIRI sensors have a high frequency of revisiting the same site and a spectral richness without equivalent. These data thus allow us the advantage that we can obtain easily an overview of the ASSS basin at regular time's step. On the other hand, many fine details of land use cannot be detected by these sensors, because of their spatial resolution (from 250 m for some MODIS products to 2,5 km for SEVIRI) (Johannes et al., 2002). These data, nevertheless, proved their utility for monitoring land use, and even for estimating water withdrawals in arid or semi-arid environment.

Thus, the imagery joint use at medium resolution (MODIS) having high temporal frequency with high resolution data (LANDSAT 5 or 8, or SPOT) and especially very high resolution (QuickBird) would allow us to conduct studies of monitoring of irrigated areas and estimating the water withdrawals more accurately at spatial and temporal scales.

There are serious scenarios to avoid, such as the soil degradation, the drought of the basin, the overconcentration of salt and its oversaturation compared to the water level, the contamination of the water by the pollution, etc.

ACKNOWLEDGMENTS

The INTERNATIONAL JOURNAL OF SCIENTIFIC AND TECHNOLOGY RESEARCH (IJSTR) published a great part of this work in August 2017, VOLUME 6, ISSUE 8. The Seventh Program, Framework for Research and Development of the European Union, coordinated by the VITO research institute (Belgium), financed the AGRICAB project by which we supported our research of which this work is a part. The African Water Facility financed the GEOAQUIFER project and the Observatory of the Sahara and the Sahel (OSS) executed it; which allowed us to know the description of the study zone. We don't forget to

acknowledge NASA permission to have the MODIS data in order to process them. The OSS's ex-Scientific and Technical former Adviser Dr. H. TREBOSSEN and the OSS's ex-Executive Director former Professor General Engineer Geographer C. FEZZANI read the paper and gave us precious advices which allowed us to improve the content.

REFERENCES

Adel Kharroubi, Soumaya Farhat, Belgacem Agoubi and Zouhir Lakhbir, "Assessment of water qualities and evidence of seawater intrusion in a deep confined aquifer: case of the coastal Djeffara Aquifer (Southern Tunisia), "Journal of Water Supply: Research and Technology-AQUA, vol. 63, no 1, pp. 76-84, 2014.

Adrian V, Rocha, Gaius RS (2009). "Advantages of a two band EVI calculated from solar and photosynthetically active radiation fluxes," Agricultural and Forest Meteorology, vol. 149, no 9, pp. 1560-1563, 2009.

Alfredo R, Huete, Kamel Didan, Yosio E (2006). Shimabukuro, Piyachat Ratana, Scott R. Saleska, Lucy R. Hutyra, Wenze Yang, Ramakrishna R. Nemani and Ranga Myneni, (2006). "Amazon rainforests green-up with sunlight in dry season," GEOPHYSICAL RESEARCH LETTERS, vol. 33, no. 6, pp. 1-4, L06405, 2006.

AYOUB A, LE QUELLEC JL, UN GRENIER FORTIFIE DANS LA DJEFFARA LIBYENNE, in : Marceau Gast, and François Sigaut, Les techniques de conservation des grains à long terme : C.N.R.S., Paris, pp. 3-18, 1981.

Cécilia B, Milena P (2012). Indicateurs de vulnérabilité / résilience du couvert végétal dérivés des données MODIS. Comparaison entre les trois sites sahéliens, Réunion ECLIS, 21 p, 2012.

Digital Globe, (2013). IKONOS. [Online] Available: https://www.digitalglobe.com/sites/default/files/DG_IKONOS_DS.pdf (2013)

EXELIS Visual Information Solutions (2012). ENVI Le logiciel leader pour l'extraction d'informations à partir de données géospatiales, 2012. [Online] Available : http://www.graphtech-gis.com/Produits_et_Services/ENVI_Exelis_VIS_Imagerie_Graphtech_Tunisie/ENVI_FR.pdf (2012)

FAO Water Development and Management Unit, (2013). FAO WATER. Software CROPWAT. [Online] Available: http://www.fao.org/nr/water/infores_databases_cropwat.html (2013)

FLASHESPACE, (2010). FLASHESPACE EN DIRECT DU CIEL ET DE L'ESPACE. SENTINEL 3, Mission opérationnelle d'océanographie et de surveillance des terres émergées. [Online] Available: http://www.flashespace.com/ (2010).

Huetea A, Didana K, Miuraa T, Rodrigueza EP, Gaoa X, Ferreirab LG (2002). "Overview of the radiometric and biophysical performance of the MODIS vegetation indices," Remote Sensing of Environment, vol. 83 , no. 1–2, pp. 195-213, 2002.

Institut Méditerranéen de l'Eau, CONSEIL GENERAL BOUCHES-DU-RHONE et Département Hérault Conseil Général, Les aquifères fossiles au sud de la Méditerranée-Etat synthétique des connaissances-Caractéristiques et contraintes d'exploitation. IME, Marseille, 30 p, 2008.

Johannes Schmetz, Paolo Pili, Stephen Tjemkes, Dieter Just, Jochen Kerkmann, Sergio Rota and Alain Ratier, "An Introduction to Meteosat Second Generation (MSG)," AMERICAN METEOROLOGICAL SOCIETY Journals, vol. 83, no 7, pp. 977-992, 2002.

Mathieu F (2014). Traitement d'Images Satellitaires S4. Ecole Nationale Supérieure Agronomique de Toulouse & Institut National Polytechnique de Toulouse, 20 p, 2014.

NASA LP DAAC, USGS EROS Center and Sioux Falls, How to interpret and use MODIS QA information in the Vegetation Indices product suite, MODIS Land Products Quality Assurance Tutorial : Part-2, 9 p, 2013.

Observatoire du Sahara et du Sahel, SYSTEME AQUIFERE DU SAHARA SEPTENTRIONAL, Une conscience de bassin, no 2. Tunis, 322 p, 2003.

Observatoire du Sahara et du Sahel, SYSTEME AQUIFERE DU SAHARA SEPTENTRIONAL, Gestion commune d'un bassin transfrontière, no 1. Tunis, 148 p, 2003.

Qiaozhen Mu, Maosheng Zhao and Steven W. Running, "Improvements to a MODIS global terrestrial evapotranspiration algorithm," Remote Sensing of Environment, vol. 115, no 8, pp. 1781-1800, 2011.